Applied Physics Letters

RESEARCH ARTICLE | APRIL 10 2024

Poling induced changes in polarization domain structure of polymer ferroelectrics for application in organic thin film transistors

Arash Ghobadi ; Somayeh Saadat Niavol ; Evan Restuccia ; Andrew C. Meng ; Suchismita Guha

Appl. Phys. Lett. 124, 153301 (2024)
https://doi.org/10.1063/5.0200724

Applied Physics Letters ARTICLE pubs.aip.org/aip/apl

Poling induced changes in polarization domain structure of polymer ferroelectrics for application in organic thin film transistors

Cite as: Appl. Phys. Lett. **124**, 153301 (2024); doi: 10.1063/5.0200724
Submitted: 28 January 2024 · Accepted: 31 March 2024 ·
Published Online: 10 April 2024

View Online Export Citation CrossMark

Arash Ghobadi, Somayeh Saadat Niavol, Evan Restuccia, Andrew C. Meng,[a] and Suchismita Guha[a]

AFFILIATIONS

Department of Physics and Astronomy, University of Missouri, Columbia, Missouri 65211, USA

[a]Authors to whom correspondence should be addressed: acmeng@missouri.edu and guhas@missouri.edu

ABSTRACT

While electrical poling of organic ferroelectrics has been shown to improve device properties, there are challenges in visualizing accompanying structural changes. We observe poling induced changes in ferroelectric domains by applying differential phase contrast (DPC) imaging in the scanning transmission electron microscope, a method that has been used to observe spatial distributions of electromagnetic fields at the atomic scale. In this work, we obtain DPC images from unpoled and electrically poled polyvinylidene fluoride trifluorethylene films and compare their performance in polymer thin film transistors. The vertically poled films show uniform domains throughout the bulk compared to the unpoled film with a significantly higher magnitude of the overall polarization. Thin film transistors comprising a donor–acceptor copolymer as the active semiconductor layer show improved performance with the vertically poled ferroelectric dielectric film compared with the unpoled ferroelectric dielectric film. A poling field of 80–100 MV/m for the dielectric layer yields the best performing transistors; higher than 100 MV/m is seen to degrade the transistor performance. The results are consistent with a reduction in deleterious charge carrier scattering from ferroelectric domain boundaries or interfacial dipoles arising from electrical poling.

High dielectric constant (κ) dielectrics, on the one hand, are favored for lowering the operating voltage of organic thin film transistors since these devices mainly work in the accumulation region; on the other hand, such dielectrics are known to reduce the carrier mobility in field-effect transistors (FETs).[1–4] The reduction in carrier mobility stems from the formation of surface Fröhlich polarons due to the polar nature of the ferroelectric dielectric, resulting in a dynamic coupling of the charge carriers. This reduction in carrier mobility is not just limited to organic FETs but has also been observed in metal oxide semiconductor FETs (MOSFETs) when high κ dielectrics such as HfO_2, ZrO_2, and Al_2O_3 are used.[5] Polymer ferroelectrics based on polyvinylidene fluoride (PVDF) are known to show polarization fluctuation dominant transport in organic FETs, where the carrier mobilities of small molecule and polymer-based FET remain unchanged with temperature as long as the dielectric is in the ferroelectric phase.[6,7]

The β phase with its all-*trans*-configuration of the carbon atoms in PVDF is ferroelectric,[8,9] but since normal casting of the films results mainly in the non-ferroelectric α phase, a copolymer of PVDF with trifluorethylene (PVDF-TrFE) is usually used in ferroelectric memory and other devices.[10–12] PVDF-TrFE films upon direct casting are already in the β phase.[13] The semicrystallinity in PVDF and its copolymers is key to its ferroelectric properties; the crystalline dipolar domains are bounded by amorphous regions. Poling, which is the application of an external electric field at the Curie temperature (ferroelectric–paraelectric transition), orients the dipoles and has been favorably exploited for enhancing transistor properties. Taking a cue from ferroelectric oxide MOSFETs, where polarization modulation in the oxide layer is seen to yield fast switching and low-power operation, polarization rotation in PVDF-TrFE based organic FETs has been explored in prior investigations.[14] What is particularly advantageous is that since organic FETs require charge accumulation at the semiconductor-dielectric interface, the dipole moment can be oriented in the vertical direction to benefit *p*- or *n*-type transport. It has been further shown that a combination of vertical and lateral poling of the PVDF-TrFE layer in organic FETs benefits from a reduction in the leakage current along with an improvement in the subthreshold swing and carrier mobility.[15]

Although poling the polymer ferroelectric layer for improving the performance of organic FETs has been demonstrated earlier, imaging the overall polarization in such bulk films has not been accomplished

before. Differential phase contrast (DPC) imaging in the Scanning Transmission Electron Microscope (STEM) has served as an important tool for observing spatial variations in specimen electromagnetic fields by measuring changes in the deflection of the electron beam. The method is well established with atomic resolution mapping of polarization domains having been demonstrated[16–18] and has been applied to a wide variety of ferroelectric materials.[19–21] While for polycrystalline ferroelectric materials, crystallographic orientation can influence beam deflection, this effect is not expected to be strong from a polymer that exhibits weak crystallinity. Particularly for thin films that are (vertically) poled in the film thickness direction, STEM DPC enables mapping ferroelectric domains in cross section view, which is the relevant specimen geometry for visualizing poling induced structural changes.[22] While DPC imaging on polymers has been shown to enhance contrast,[23,24] application to characterize ferroelectric domains in polymers (*vide infra*) remains untapped. This characterization provides an opportunity for systematic study of the structure–property relationship in ferroelectric polymers.

Here, we use a donor–acceptor copolymer based on the acceptor unit diketopyrrolopyrrole (DPP) and the donor moiety of dithienylthieno[3,2-b]thiophene (DTT) (DPP-DTT) as the active semiconducting layer and a 75:25 ratio PVDF-TrFE as the dielectric film in a bottom-gate, top-contact FET architecture. Prior to spincoating the DPP-DTT film, the spincoated PVDF-TrFE layer was externally poled in the vertical direction at fields varying from 60 to 300 MV/m, as schematically shown in Fig. 1(a). Details are provided in the supplementary material. The poling was carried out in such a way that the dipole moment points vertically downward [Fig. 1(b)], which ensures that the majority charge carriers, holes in this case, accumulate more easily at the semiconductor-dielectric interface. Our earlier work has shown that small molecule based FETs, where the semiconducting layer is more crystalline, benefit from such vertical poling in the PVDF-TrFE layer;[14] however, what is not known is how the polarization domains are oriented and the extent of the polarization when the dielectric layer is poled. We note that the unpoled PVDF-TrFE layer is already in the ferroelectric phase but since some of the domains are randomly oriented, the extent of the polarization in the bulk of the film is expected to be less compared with a poled film.

Figures 1(c) and 1(d) show the top view and cross-sectional scanning electron microscope (SEM) images of the DPP-DTT/PVDF-TrFE FET, respectively. The channel length for this device is 100 μm. The cross-sectional image clearly shows that the PVDF-TrFE layer, as marked by the red lines, is approximately 125 nm thick. These images are from an unpoled device; however, the poled device shows a similar contrast. Cross-sectional SEM imaging is unable to differentiate between poled and unpoled polymer ferroelectric films. The contrast mechanism arising from the electric polarization in DPC/STEM images provides an ideal tool for comparing the two films.

STEM imaging was used to characterize PVDF-TrFE thin films. We note that the STEM data were taken at a high acceleration voltage of 300 kV, which results in a significantly lower scattering cross section and has been reported to reduce electron interactions with beam-sensitive materials such as zeolites.[25,26] The fields of view used for imaging were larger than 200 nm, and dwell times of up to 32 μs were used with beam currents of up to ~200 pA. A schematic showing the contrast mechanism for DPC imaging of ferroelectric domains is shown in Fig. 2(a). While the DPC in the PVDF-TrFE [region between two red marked lines in Figs. 2(c) and 2(e)] is related to electrical polarization induced deflections of the electron beam, the DPC in the top and bottom electrodes, which are polycrystalline, arises mainly due to crystallographic orientation differences[19,27] and is not indicative of an electric polarization as metals cannot support an electric potential difference (above the top red line and below the bottom red line). In DPC images, polarization orientation and magnitude are indicated by color and intensity, respectively, with yellow-green corresponding to up and blue-magenta corresponding to down. The poling field for the vertically poled PVDF-TrFE film was 100 MV/m. Figures 2(d) and 2(e) show a high-angle annular dark-field (HAADF) STEM image and

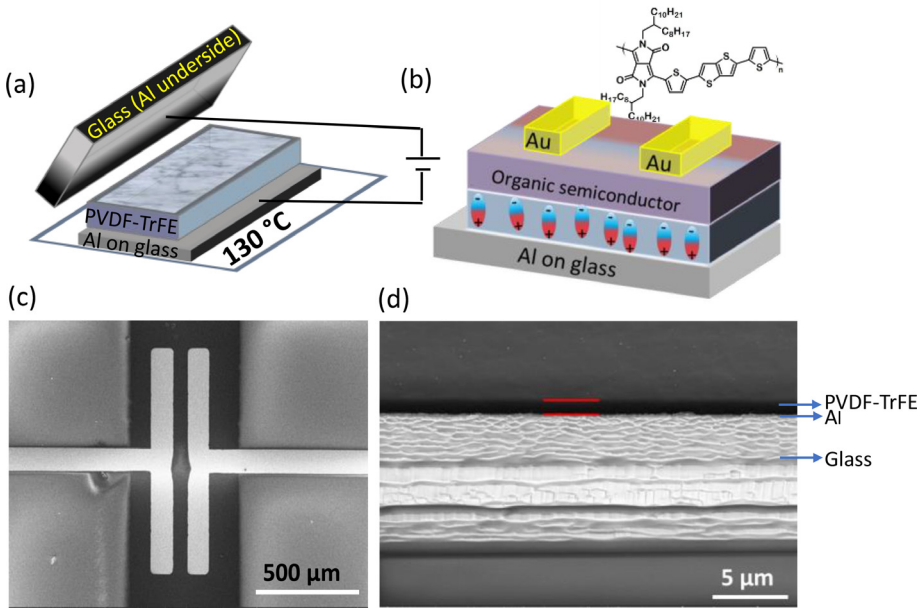

FIG. 1. (a) Schematic of the electrical poling process in a film of PVDF-TrFE deposited on top of Al-coated glass. (b) Schematic of the thin film transistor using vertically poled PVDF-TrFE, where the net dipole moment points downward. (c) SEM image of the top view of the transistor with Au source/drain contacts. The channel length was 100 μm. (d) Cross-sectional SEM image of the FET where the PVDF-TrFE layer (of thickness 125 nm) is marked by the red horizontal lines.

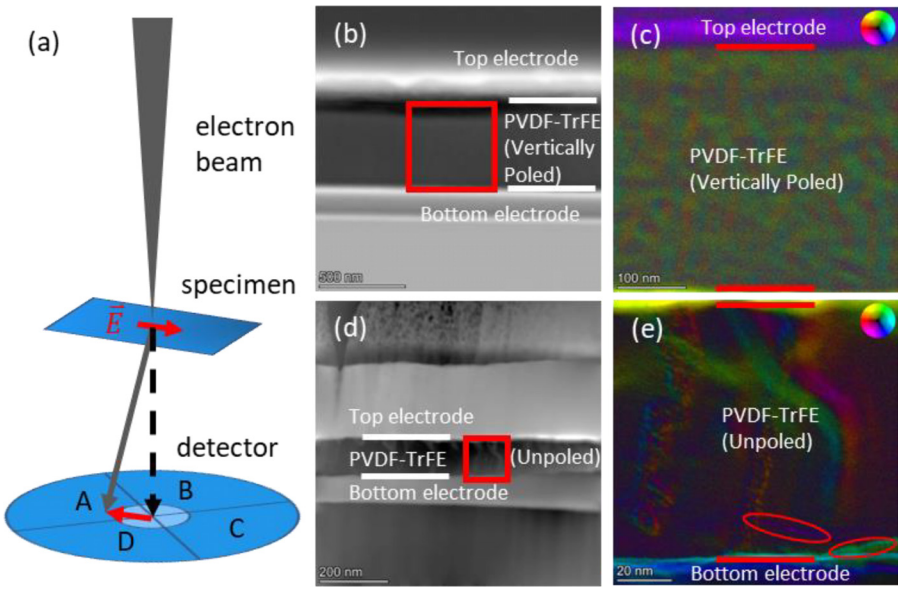

FIG. 2. (a) Schematic of contrast mechanism in DPC STEM image. (b) HAADF STEM and (c) DPC STEM image of vertically poled PVDF-TrFE. (d) HAADF STEM and (e) DPC STEM image of unpoled PVDF-TrFE with high polarization regions at the bottom electrode/PVDF-TrFE interface circled in red.

a DPC STEM image of unpoled PVDF-TrFE, respectively. Darker contrast (low intensity) in large areas of the DPC image of unpoled PVDF-TrFE is consistent with either low polarization magnitude or polarization orientation in the in-plane direction parallel to the electron beam. On the other hand, the polarization is higher at the unpoled PVDF-TrFE/electrode interfaces [Fig. 2(e), circled regions]. Polarization domains in unpoled PVDF-TrFE are approximately columnar but are not vertical throughout. Figures 2(b) and 2(c) show a HAADF STEM image and a DPC STEM image of vertically poled PVDF-TrFE, respectively. In contrast, the DPC image of the vertically poled sample shows significantly more uniform contrast with larger areas where the polarization is in the up direction. This is consistent with expectations that polarization domains align with the poling electric field.[15] Also, the PVDF-TrFE/electrode interfaces do not show higher polarization as observed in the unpoled sample.

We compare unpoled and vertically poled PVDF-TrFE with DPP-DTT as the active layer in FET architectures. The vertical poling was carried out at four different fields between 60 and 300 MV/m. Figure 3 shows the transfer and output characteristics from unpoled and poled devices (60 and 100 MV/m). The saturation carrier mobility $\mu_{sat} = \frac{2L}{WC_i}\left(\frac{\partial\sqrt{I_D}}{\partial V_{GS}}\right)^2$ is determined from the transfer characteristics by measuring the drain current (I_D) as the gate source voltage (V_{GS}) is swept by keeping the drain-source voltage (V_{DS}) constant in the saturation region. The channel length (L) and width (W) were identical for the three devices, and the capacitance of the dielectric (C_i) was measured from metal-PVDF-TrFE-metal structures. Upon vertically poling the ferroelectric film at 100 MV/m, μ_{sat} increases by more than twice compared with the unpoled film. In each of these cases, we find the threshold voltage (V_{th}) to be negative, which is often seen in organic FETs and is a sign of gate bias dependent mobility.[28] The modulation in the output characteristics significantly improves upon vertical poling.

Our prior work with small molecules (DNTT, pentacene, and TIPS-pentacene) showed a dramatic improvement in the subthreshold swing ($SS = [\partial \log I_D/\partial V_{GS}]^{-1}$) upon vertically poling the PVDF-TrFE film,[14] which is not the case here with DPP-DTT. The semiconductor-dielectric interface plays a large role in reducing SS; small molecules being more crystalline seem to benefit from the polarized domains of the ferroelectric layer at the interface compared with polymers such as DPP-DTT.

Figure 4(a) shows the transfer characteristics from three different FETs (same W/L ratio), where the PVDF-TrFE layer was poled at different voltages. In addition to an improvement in the carrier mobility with increasing the poling voltage, V_{th} decreases from −7.5 V for the 60 MV/m device to −2.3 V when the poling voltage is increased to 80 MV/m. As pointed out earlier, a negative V_{th} in p-type organic FETs is a signature of gate bias dependent mobility, which is an indication of polaronic transport. Poling, which increases the overall polarization magnitude and the size of domains in the ferroelectric, thus, reduces the polarization fluctuation dominant transport, as evident from a lower threshold voltage and enhanced carrier mobility. This is also consistent with our observation that polarization domains in PVDF-TrFE are both larger and more uniform after vertical poling than in as-deposited thin films. Evidence of polarization fluctuation dominant transport in unpoled PVDF-TrFE/DPP-DTT FET is shown in the supplementary material.

Furthermore, we have investigated the impact of increasing the poling voltage on the FET properties. Figure 4(b) displays the transfer and the output characteristics from a device where the PVDF-TrFE layer was poled to a voltage of 300 MV/m. A degradation of the on/off ratio and the output characteristics are evident. A higher off current suggests a spontaneous polarization field in the lateral direction, which may arise from some polarization domains being oriented in the direction of the source/drain contacts. These results suggest that there is an optimal vertical poling voltage (∼100 MV/m) of the PVDF-TrFE layer that enhances the FET properties.

Unlike thin PVDF-TrFE films, which show needlelike grain morphology upon annealing,[29,30] the thicker PVDF-TrFE films used in this study do not show any grain-like morphology as reported in Ref. 14.

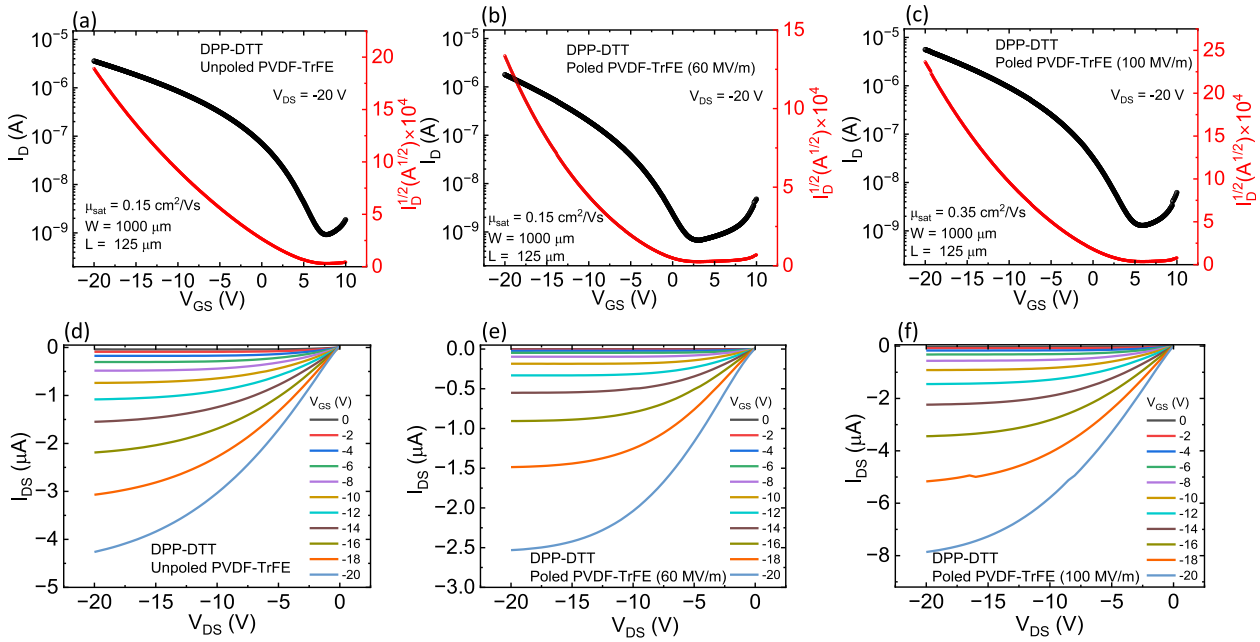

FIG. 3. FET characteristics from unpoled and poled DPP-DTT/PVDF-TrFE FETs. (a)–(c) Transfer and (d)–(f) output characteristics of unpoled and poled PVDF-TrFE (60 and 100 MV/m) FETs, respectively. The W/L ratios for all devices are 8.

Comparing STEM DPC data from unpoled and vertically poled PVDF-TrFE, vertical poling appears to increase not only the magnitude of the polarization but also the ferroelectric domain size. Prior SEM and x-ray diffraction results revealed that vertical poling is associated with domains $> 1\,\mu$m along with higher crystallinity of the PVDF-TrFE film.[14] Combined with the observed increase in mobility of vertically poled devices, this could be consistent with a decrease in deleterious charge carrier scattering at ferroelectric domain boundaries.[31] For example, domain wall and polarization mediated transport may be convoluted with free charge carrier motion. Another possibility is that the observation is related to poling induced differences in polarization at the PVDF-TrFE/electrode interface. As the observed DPC at the interface could arise from an interfacial dipole, the increase in mobility due to poling is consistent with reduced dipole scattering of charge carriers.[32–34] Either of these effects can increase the charge carrier lifetime, leading to the observed increase in mobility. Visualization of ferroelectric domains in unpoled and poled PVDF-TrFE, therefore, provides a unique opportunity to investigate the structural origins of ferroelectric polymer device behavior.

As a further check for understanding enhanced carrier mobilities in the poled PVDF-TrFE compared with the unpoled ferroelectric, we have carried out detailed analysis of the trap density of states (DOS) using the Grünewald's method.[35,36] Since this method requires the transfer characteristics from a single linear region at room temperature, it has been extensively used for determining the trap DOS in organic FETs.[37,38] Briefly, the dielectric–semiconductor interface potential, $V_0(U_{GS})$, is first determined from the dependence of I_{DS} on the electric field due to V_{GS}, where $U_{GS} = |V_{GS}\text{-}V_{FB}|$ with V_{FB} being the flatband voltage. From V_0 as a function of U_{GS}, one can then determine the carrier (hole) density as $p(V_0) = \frac{\varepsilon_0 \varepsilon_i^2}{\varepsilon_s l^2 e} U_{GS} \left(\frac{dV_0}{dU_{GS}}\right)^{-1}$, where ε_s and ε_i are the dielectric constants of the semiconductor and the insulator,

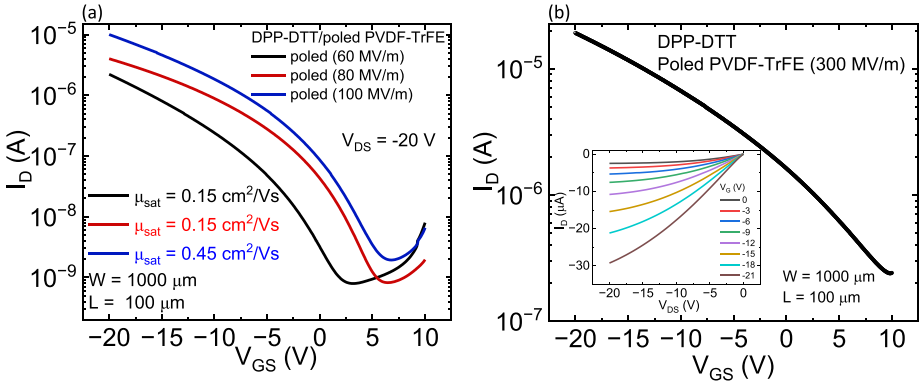

FIG. 4. (a) Transfer characteristics of three different DPP-DTT/PVDF-TrFE FETs where the poling of the PVDF-TrFE layer was carried out at three different fields: 60, 80, and 100 MV/m. (b) Transfer and output (inset) characteristics of a DPP-DPP/PVDF-TrFE FET where the vertical poling was carried out at 300 MV/m.

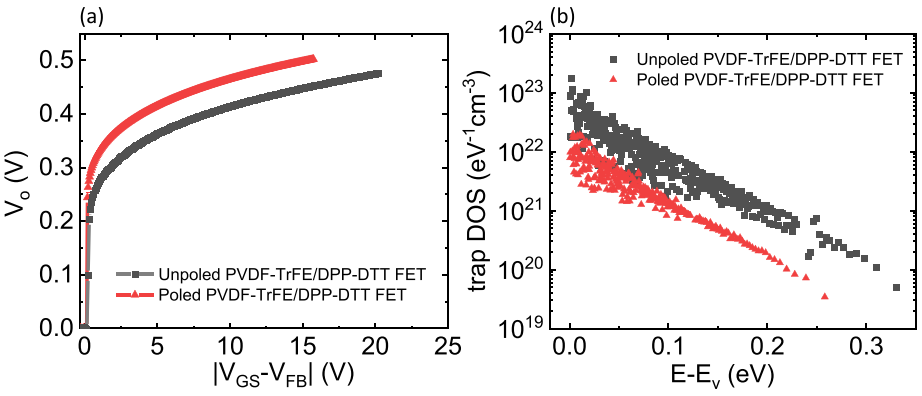

FIG. 5. (a) The interface potential vs $U_{GS} = |V_{GS}\text{-}V_{FB}|$ above the flatband voltage for unpoled and poled DPP-DTT/PVDF-TrFE FETs. The poling field was 100 MV/m. (b) Trap DOS in poled and unpoled DPP-DTT/PVDF-TrFE FETs vs $E\text{-}E_v$.

respectively, ε_0 is the permittivity of free space, and l is the thickness of the dielectric layer. The trap DOS ($N(E)$) is then obtained from $N(E) \approx \frac{1}{e}\frac{dp(V_0)}{dV_0}$. Details of this method are provided in the supplementary material.

Figures 5(a) and 5(b) show the interface potential and the calculated trap DOS for DPP-DTT FETs with poled (100 MV/m) and unpoled PVDF-TrFE, respectively. As outlined in the supplementary material, the interface potential was obtained using numerical methods using an open-source Python library from the FET transfer characteristics (in the linear region). V_{FB} was assumed to be the turn-on voltage of the transistor. The valence band energy (E_v) is estimated from the effective mobility vs V_{GS} and is taken at the voltage where the mobility saturates.[37] The trap DOS is seen to be almost an order of magnitude lower for the poled PVDF-TrFE FET, which corroborates the higher performance of the transistor compared with the unpoled device.

In summary, we used STEM DPC to characterize ferroelectric domains in unpoled and vertically poled PVDF-TrFE thin films that were used to fabricate transistor devices. We observed increased polarization magnitude and uniformity in poled samples. While some polarization domains in the unpoled film are localized near the PVDF-TrFE/bottom electrode interface, poling homogenizes the distribution of the domains. Concurrent with increased mobility in the poled samples, the results seem to be consistent with decreased charge carrier scattering at ferroelectric domains or from interfacial dipoles or a combination of both, which further correlates with lower trap DOS. The lower trap DOS is most likely a manifestation of higher crystallinity in the vertically poled device. STEM DPC is promising for characterizing the structure–property relationship of ferroelectric polymers. DPC imaging of polymer ferroelectrics, in the future, may be promising for *in situ* electrical poling experiments to study domain dynamics in real time.

See the supplementary material for details on device fabrication, characterization techniques including electrical measurements and electron microscopy, temperature-dependent carrier mobility, and Grünewald's method.

We acknowledge support of this work through the U.S. National Science Foundation (NSF) under Grant No. ECCS-2324839.

AUTHOR DECLARATIONS

Conflict of Interest

The authors have no conflicts to disclose.

Author Contributions

Arash Ghobadi: Data curation (equal); Formal analysis (lead); Investigation (equal); Methodology (equal); Writing – original draft (supporting); Writing – review & editing (supporting). **Somayeh Saadat Niavol:** Data curation (equal); Formal analysis (supporting); Writing – original draft (supporting); Writing – review & editing (supporting). **Evan Restuccia:** Formal analysis (supporting); Software (lead); Writing – original draft (supporting); Writing – review & editing (supporting). **Andrew C. Meng:** Conceptualization (equal); Data curation (equal); Formal analysis (equal); Investigation (equal); Methodology (equal); Writing – original draft (equal); Writing – review & editing (equal). **Suchismita Guha:** Conceptualization (lead); Data curation (supporting); Funding acquisition (lead); Investigation (supporting); Project administration (lead); Supervision (equal); Writing – original draft (lead); Writing – review & editing (lead).

DATA AVAILABILITY

The data that support the findings of this study are available from the corresponding authors upon reasonable request.

REFERENCES

[1]I. N. Hulea, S. Fratini, H. Xie, C. L. Mulder, N. N. Iossad, G. Rastelli, S. Ciuchi, and A. F. Morpurgo, "Tunable Frohlich polarons in organic single-crystal transistors," Nat. Mater. **5**(12), 982–986 (2006).
[2]H. Houili, J. D. Picon, L. Zuppiroli, and M. N. Bussac, "Polarization effects in the channel of an organic field-effect transistor," J. Appl. Phys. **100**(2), 023702 (2006).
[3]A. Laudari and S. Guha, "Temperature dependent carrier mobility in organic field-effect transistors: The role of dielectrics," J. Appl. Phys. **125**(3), 035501 (2019).
[4]A. Laudari, J. Barron, A. Pickett, and S. Guha, "Tuning charge transport in PVDF-based organic ferroelectric transistors: Status and outlook," ACS Appl. Mater. Interfaces **12**(24), 26757–26775 (2020).
[5]M. V. Fischetti, D. A. Neumayer, and E. A. Cartier, "Effective electron mobility in Si inversion layers in metal–oxide–semiconductor systems with a high-κ insulator: The role of remote phonon scattering," J. Appl. Phys. **90**(9), 4587–4608 (2001).
[6]S. P. Senanayak, S. Guha, and K. S. Narayan, "Polarization fluctuation dominated electrical transport processes of polymer-based ferroelectric field effect transistors," Phys. Rev. B **85**(11), 115311 (2012).

[7]A. Laudari and S. Guha, "Polarization-induced transport in ferroelectric organic field-effect transistors," J. Appl. Phys. **117**(10), 105501 (2015).
[8]R. G. Kepler and R. A. Anderson, "Ferroelectricity in polyvinylidene fluoride," J. Appl. Phys. **49**(3), 1232–1235 (1978).
[9]A. J. Lovinger, "Ferroelectric polymers," Science **220**(4602), 1115–1121 (1983).
[10]R. C. G. Naber, C. Tanase, P. W. M. Blom, G. H. Gelinck, A. W. Marsman, F. J. Touwslager, S. Setayesh, and D. M. de Leeuw, "High-performance solution-processed polymer ferroelectric field-effect transistors," Nat. Mater. **4**(3), 243–248 (2005).
[11]Y. Wang, X. Huang, T. Li, L. Li, X. Guo, and P. Jiang, "Polymer-based gate dielectrics for organic field-effect transistors," Chem. Mater. **31**(7), 2212–2240 (2019).
[12]B. Stadlober, M. Zirkl, and M. Irimia-Vladu, "Route towards sustainable smart sensors: Ferroelectric polyvinylidene fluoride-based materials and their integration in flexible electronics," Chem. Soc. Rev. **48**(6), 1787–1825 (2019).
[13]G. Knotts, A. Bhaumik, K. Ghosh, and S. Guha, "Enhanced performance of ferroelectric-based all organic capacitors and transistors through choice of solvent," Appl. Phys. Lett. **104**(23), 233301 (2014).
[14]A. Laudari, A. R. Mazza, A. Daykin, S. Khanra, K. Ghosh, F. Cummings, T. Muller, P. F. Miceli, and S. Guha, "Polarization modulation in ferroelectric organic field-effect transistors," Phys. Rev. Appl. **10**(1), 014011 (2018).
[15]A. Laudari, A. Pickett, F. Shahedipour-Sandvik, K. Hogan, J. E. Anthony, X. He, and S. Guha, "Textured poling of the ferroelectric dielectric layer for improved organic field-effect transistors," Adv. Mater. Interfaces **6**(4), 1801787 (2019).
[16]N. Shibata, S. D. Findlay, Y. Kohno, H. Sawada, Y. Kondo, and Y. Ikuhara, "Differential phase-contrast microscopy at atomic resolution," Nat. Phys. **8**(8), 611–615 (2012).
[17]M. Campanini, K. Eimre, M. Bon, C. A. Pignedoli, M. D. Rossell, and R. Erni, "Atomic-resolution differential phase contrast STEM on ferroelectric materials: A mean-field approach," Phys. Rev. B **101**(18), 184116 (2020).
[18]T. Seki, Y. Ikuhara, and N. Shibata, "Toward quantitative electromagnetic field imaging by differential-phase-contrast scanning transmission electron microscopy," Microscopy **70**(1), 148–160 (2020).
[19]L. Chen, Z. Liang, S. Shao, Q. Huang, K. Tang, and R. Huang, "First direct observation of the built-in electric field and oxygen vacancy migration in ferroelectric $Hf_{0.5}Zr_{0.5}O_2$ film during electrical cycling," Nanoscale **15**(15), 7014–7022 (2023).
[20]X. Zhang, E. A. Stach, W. J. Meng, and A. C. Meng, "Nanoscale compositional segregation in epitaxial AlScN on Si (111)," Nanoscale Horiz. **8**(5), 674–684 (2023).
[21]X. Zhang, W. Xu, W. J. Meng, and A. C. Meng, "Single crystal ferroelectric AlScN nanowires," CrystEngComm **26**(2), 180–191 (2024).
[22]Q. Huang, Z. Chen, M. J. Cabral, F. Wang, S. Zhang, F. Li, Y. Li, S. P. Ringer, H. Luo, Y.-W. Mai, and X. Liao, "Direct observation of nanoscale dynamics of ferroelectric degradation," Nat. Commun. **12**(1), 2095 (2021).
[23]S. Inamoto, A. Yoshida, and Y. Otsuka, "Three-dimensional analysis of non-stained polymer alloy using differential phase contrast-STEM tomography," Microsc. Microanal. **25**(S2), 1826–1827 (2019).
[24]S. Inamoto, S. Shimomura, and Y. Otsuka, "Electrostatic potential imaging of phase-separated structures in organic materials via differential phase contrast scanning transmission electron microscopy," Microscopy **69**(5), 304–311 (2020).
[25]K. Yoshida and Y. Sasaki, "Optimal accelerating voltage for HRTEM imaging of zeolite," Microscopy **62**(3), 369–375 (2012).
[26]O. Ugurlu, J. Haus, A. A. Gunawan, M. G. Thomas, S. Maheshwari, M. Tsapatsis, and K. A. Mkhoyan, "Radiolysis to knock-on damage transition in zeolites under electron beam irradiation," Phys. Rev. B **83**(11), 113408 (2011).
[27]C. Ophus, "Four-dimensional scanning transmission electron microscopy (4D-STEM): From scanning nanodiffraction to ptychography and beyond," Microsc. Microanal. **25**(3), 563–582 (2019).
[28]G. Horowitz, "Organic field-effect transistors," Adv. Mater. **10**(5), 365–377 (1998).
[29]D. Guo, I. Stolichnov, and N. Setter, "Thermally induced cooperative molecular reorientation and nanoscale polarization switching behaviors of ultrathin poly (vinylidene fluoride-trifluoroethylene) films," J. Phys. Chem. B **115**(46), 13455–13466 (2011).
[30]D. Guo and N. Setter, "Impact of confinement-induced cooperative molecular orientation change on the ferroelectric size effect in ultrathin P(VDF-TrFE) films," Macromolecules **46**(5), 1883–1889 (2013).
[31]R. K. Vasudevan, W. Wu, J. R. Guest, A. P. Baddorf, A. N. Morozovska, E. A. Eliseev, N. Balke, V. Nagarajan, P. Maksymovych, and S. V. Kalinin, "Domain wall conduction and polarization-mediated transport in ferroelectrics," Adv. Funct. Mater. **23**(20), 2592–2616 (2013).
[32]J. Appel and W. B. Teutsch, "Electric dipole scattering in nonpolar semiconductors," J. Phys. Chem. Solids **23**(11), 1521–1524 (1962).
[33]W. Zhao and D. Jena, "Dipole scattering in highly polar semiconductor alloys," J. Appl. Phys. **96**(4), 2095–2101 (2004).
[34]T. Hatakeyama, H. Hirai, M. Sometani, D. Okamoto, M. Okamoto, and S. Harada, "Dipole scattering at the interface: The origin of low mobility observed in SiC MOSFETs," J. Appl. Phys. **131**(14), 145701 (2022).
[35]M. Grünewald, P. Thomas, and D. Würtz, "A simple scheme for evaluating field effect data," Phys. Status Solidi B **100**(2), K139–K143 (1980).
[36]W. L. Kalb and B. Batlogg, "Calculating the trap density of states in organic field-effect transistors from experiment: A comparison of different methods," Phys. Rev. B **81**(3), 035327 (2010).
[37]M. Geiger, L. Schwarz, U. Zschieschang, D. Manske, J. Pflaum, J. Weis, H. Klauk, and R. T. Weitz, "Quantitative analysis of the density of trap states in semiconductors by electrical transport measurements on low-voltage field-effect transistors," Phys. Rev. Appl. **10**(4), 044023 (2018).
[38]D. Dremann, E. J. Kumar, K. J. Thorley, E. Gutiérrez-Fernández, J. D. Ververs, J. D. Bourland, J. E. Anthony, A. R. S. Kandada, and O. D. Jurchescu, "Understanding radiation-generated electronic traps in radiation dosimeters based on organic field-effect transistors," Mater. Horiz. **11**(1), 134–140 (2024).